Controlled Intracellular Generation of Reactive Oxygen Species in Human Mesenchymal Stem Cells Using Porphyrin Conjugated Nanoparticles

Andrea S. Lavado,[a] Veeren M. Chauhan,[a] Amer Alhaj Zen,[b] Francesca Giuntini,[c] Rhodri E. Jones,[a] Ross W. Boyle,[c] Andrew Beeby,[d] Weng. C. Chan[b] and Jonathan W. Aylott[a*]

[a *]Laboratory of Biophysics and Surface Analysis, School of Pharmacy, Boots Science Building, University of Nottingham, Nottingham, NG7 2RD, UK. E-mail: Jon.Aylott@nottingham.ac.uk
Tel: +44 (0) 115 9516229
[b]School of Pharmacy, Centre for Biomolecular Sciences, University of Nottingham, Nottingham, NG7 2RD, UK
[c] University of Hull, Department of Chemistry, Hull, HU6 7RX, UK.
[d] University of Durham, Department of Chemistry, Durham, DH1 3LE, UK

Abstract

Nanoparticles capable of generating controlled amounts of intracellular reactive oxygen species (ROS) were synthesized by functionalizing polyacrylamide nanoparticles with Zinc (II) porphyrin photosensitisers. Controlled ROS production was demonstrated in human mesenchymal stem cells (hMSCs) through 1) production of nanoparticles functionalized with varying percentages of Zinc (II) porphyrin and 2) modulating the number of doses of excitation light to internalized nanoparticles. hMSCs treated with nanoparticles functionalized with increasing percentages of Zn(II) porphyrin and high number of irradiations of excitation light were found to generate greater amounts of ROS. A novel dye, which is transformed into a fluorescent entity in the presence of hydrogen peroxide, provided an indirect indicator for cumulative ROS production. The mitochondrial membrane potential was monitored to investigate the destructive effect of increased intracellular ROS production. Flow cytometric analysis of nanoparticle treated hMSCs suggested irradiation with excitation light signalled controlled apoptotic cell death, rather than uncontrolled necrotic cell death. Increased intracellular ROS production did not induce phenotypic changes in hMSC subcultures. Zn (II) porphyrin functionalised nanoparticles could find broad utility in stimulation of intracellular oxidative stress and communication.

Introduction

Reactive oxygen species (ROS) form through conversion of molecular oxygen, by either (Type I) electron transfer, to produce superoxide, hydrogen peroxide (H_2O_2) and hydroxyl radicals or, (Type II) energy transfer, to produce singlet oxygen.[1] At a cellular level ROS production is highly regulated, typically through confinement of their production to specific organelles, such as the mitochondria,[2] and management of overproduction with antioxidants.[3] Controlled ROS production is known to regulate processes, such as programmed cell death,[4] initiation of host defences to pathogens[5] and production of energy *via* the mitochondrial electron transport chain.[6] Uncontrolled ROS production can propagate chain reactions that can cause irreversible damage to intracellular nucleic acids,[7] proteins[8] and lipids[9] that can result in cellular necrosis,[10] neoplastic mutations[11] and neurodegenerative disorders.[12]

The effects of ROS on intracellular processes have been investigated through exogenous addition of H_2O_2.[13, 14] However, diffusion of H_2O_2 through cell membranes is thought to be restricted,[15] due to tightly regulated membrane channels, such that the effect of exogenous ROS on intracellular effects can be misinterpreted.[16] Therefore, artificially stimulating intracellular ROS, independent of innate and exogenous ROS, in a controlled manner would enhance the understanding of how oxidative stress contributes to healthy or diseased states.

Polyacrylamide nanoparticles are at the forefront of investigating cellular microenvironments of interest.[17] Due to their 1) small size, 2) optical transparency, 3) large surface to volume ratio, and 4) highly versatile matrix, which can be readily engineered to control physicochemical parameters, they can be delivered to biological systems with minimal perturbation.[18] We and others have shown previously how polyacrylamide nanoparticles can be utilized as an analytical tool[19-22] to target subcellular spaces[23-25] and provide a real-time measurements of the role of key biological parameters *in situ*.[26]

More recently, polyacrylamide nanoparticles have been used as a drug delivery tool for photodynamic therapy[27] that utilise photoexcitable compounds that cause extensive tissue damage when irradiated with excitation light. The damage is inflicted through the generation of ROS, when excited photosensitizers come into contact with biological systems. Porphyrins are examples of photosensitisers that have been extensively used to treat diseased tissue.[28] They are composed of a sixteen membered aromatic ring, synthesised through condensation of substituted pyrroles, to produce a planar structure. The planar structure can be used to stabilise metal complexes, usually with a 2+ valency, which dictate the photo excitable properties of the porphyrin. [29]

This article describes the synthesis and characterization of polyacrylamide nanoparticles conjugated to Zinc (II) or Copper (II) complexed porphyrins. Nanoparticles were doped with cationic chemical groups, to improve sub-cellular localization[30] and delivered to human mesenchymal stem cells (hMSCs). Control over ROS generation was demonstrated by: (1) attenuating the percentage of porphyrins on the nanoparticle surface and (2) modulating the number of light doses to the internalized nanoparticles. The degree of ROS production was visualized through use of a newly synthesized dye, which is chemically transformed into a fluorescent entity in the presence of ROS. The cytotoxic effects and possible phenotypic changes, induced by intracellular ROS generation, on hMSCs were investigated using flow cytometry.

Results and Discussion

Synthesis and Characterisation of Porphyrin Functionalised Nanoparticles

Two porphyrins with different metal complexes, Zn (II) and Cu (II), were utilised as part of this study, Scheme 1.[31] Porphyrins with Zn (II) have been shown to generate ROS, whereas, porphyrins with Cu (II) do not demonstrate ROS production.[32] The difference in activity is due to the electronic properties of the metal ions. When excited, porphyrins with Zn (II) permit intersystem crossing of electrons to the triplet state and demonstrate photosensitising activity. Porphyrins with Cu (II) do not permit intersystem crossing of excited electrons and as a result do not possess enough energy to produce photosensitising activity. Due to the differences in activity the Cu (II) porphyrin functionalised nanoparticles were utilised as a control, so that the photosensitising activity could be attributed to the Zn (II) porphyrin functionalised nanoparticles alone.

Porphyrins were covalently linked to nanoparticles via a Cu (I)-catalysed alkyne-azide cycloaddition reaction.[31] The percentage of nanoparticle functionalization was determined by titrating alkyne functionalised nanoparticles with porphyrin azides. Nanoparticles saturated with porphyrin were considered to be 100 % functionalised. Nanoparticles functionalised with 5 %, 10 % and 20 % Zn(II) or Cu (II) porphyrins were prepared with nanoparticle diameters centred at 80 nm (ranging between 10 and 100 nm) and positive surface charge (zeta potential > +15 mV) (see supporting information Figure S2 and S3).

Delivery of Porphyrin Functionalised Nanoparticles

Mitochondria are known as the major source of ROS within cells. Therefore, it is highly desirable for tools engineered to trigger the production of ROS, like the porphyrin functionalised nanoparticles presented here, to preferentially target the mitochondria. To determine the subcellular localisation of the nanoparticles, co-localisation analyses were performed on hMSCs treated with Zn (II) porphyrin (5%) functionalised nanoparticles, and stained with LysoTracker® blue and MitoTracker® Green.

Figure 1A shows a representative merged channel image of Zn (II) porphyrin functionalised nanoparticles delivered to hMSCs. The insets show the individual channels; (A*i*) brightfield, (A*ii*) blue (LysoTracker®), (A*iii*) green (MitoTracker®) and (A*iv*) red fluorescent channels (Zn (II) porphyrin conjugated nanoparticles). Separation of the fluorescence channels to observe co-localisation of Zn (II) porphyrin functionalised nanoparticles with the mitochondria, Figure 1B, and lysozymes, Figure 1C, facilitates characterisation of the subcellular location.

The lysozymes, as highlighted by LysoTracker® blue, appear in punctate vesicles that are co-localised in regions with Zn (II) porphyrin functionalised particles (Figure 1B, *purple*). The nanoparticles are internalized efficiently as highlighted by the strong signal observed in the red fluorescence channel (Figure 1A*iv*). The mitochondria, identified by MitoTracker® green, are distributed throughout the cytoplasm and are also co-localised with Zn (II) porphyrin conjugated nanoparticles (Figure 1C). The images comprising Figure 1 indicate porphyrin functionalised nanoparticles are internalised and preferentially associate with mitochondria, although not exclusively, over lysozymes.

Fluorescence Imaging ROS Production

A novel dye, 7-(4,4,5,5-tetramethyl-1,3,2-dioxaborolan-2-yl)-4-(trifluoromethyl)-2H-chromen-2-one (BPTFMC), was used to deterimine the ability of the Zn(II) porphyrin functionalised nanoparticles to generate ROS. BPTFMC is transformed in the presence of hydrogen peroxide (H_2O_2) to the fluorescent entity 7-hydroxy-4-(trifluoromethyl)-2H-chromen-2-one (HTFMC), Scheme 2. Visulisation of HTFMC fluorescence in subcellular spaces can therefore be utilised as an indirect indicator for cumulative ROS production (see supporting information Figures S6-S8).

Controlled ROS generation in hMSCs

Controlled ROS production in hMSCs was demonstrated through: 1) irradiation of internalised nanoparticles with increasing percentages of Zn (II) porphyrin (5 %, 10 % and 20 %), with a single dose of excitation light and 2) irradiation of internalised nanoparticles, functionalised with 5% Zn(II) porphyrin, with repeated doses of excitation light.

<u>Effect of increases in the percentage of Zn (II) porphyrin functionalisation</u>

The effect of a single dose of excitation light on internalised nanoparticles bearing 5 %, 10 % and 20 % of Zn(II) porphyrin was investigated. hMSCs were treated with nanoparticle suspensions after which they were thoroughly washed to remove non-internalised nanoparticles then stained with BPTFMC and MitoTracker® red; to observe ROS production events and location of viable mitochondria in sub-cellular spaces, respectively.

After irradiation with a single dose of light (512 µW, 8mm^2, 2 seconds), an increase in the fluorescence intensity from HTMFC (*blue*) was observed, which correlates with percentage increases in Zn (II) porphyrin conjugated to the nanoparticle, Figure 2. The extent of cytotoxicity caused by the ROS production was demonstrated by the fluorescence response from MitoTracker® red, which emits a fluorescence response when bound to viable mitochondrial membranes with active membrane potentials.[33] Figure 2 highlights the presence of a 'blast zone' within which substantial amounts ROS has been produced, whilst the number of cells with active mitochondrial membrane potentials has been considerably reduced. The extent of the lethality of high percentages of Zn (II) porphyrin is demonstrated by hMSCs treated with 20 % Zn(II) porphyrin, which show a clear perimeter between viable and non-viable cells. Therefore, the extent of ROS production and consequential cytotoxicity, as indicated by enhanced HTFMC and diminished MitoTraker® red fluorescence, respectively, is profoundly influenced by increases in the percentage of porphyrin functionalization.

<u>Effect of repeat doses of excitation light to produce ROS</u>

A single dose of excitation light produced subtle increases in ROS for hMSCs treated with nanoparticles functionalised with 5% Zn (II) porphyrin, Figure 2. To investigate if ROS production can be augmented in a controlled manner, internalised nanoparticles functionalised with 5% Zn (II) porphyrin were subjected to repeat doses of excitation light. hMSCs were irradiated with a dose of excitation light every 5 minutes for 100 minutes. The progress of cellular events was captured at 5, 30, 60 and 100 minutes, corresponding to 1, 6, 12 and 20 irradiations, respectively, Figure 3.

hMSCs treated with 5% Cu(II) functionalised porphyrins show no observable differences in cellular morphology, increases in ROS production or cytotoxicity after 20 irradiations, as indicated by brightfield images, absence of HTFMC fluorescence and similarity of fluorescence emission from mitrotracker red across all time points, respectively. This observation is also true for hMSCs treated with nanoparticles functionalised with 5% Zn(II) porphyrin after a single dose of excitation light.

The first signs of ROS generation appear after 6 irradiations for hMSCs treated with 5% Zn(II) functionalised nanoparticles, Figure 3 (*blue*). At these low levels of ROS, there are no apparent changes in cellular toxicity, as there are no noticeable changes in cellular morphology or fluorescence intensity from MitoTracker® red. After 12 irradiations, ROS production and its cytotoxic effects are evident, as the fluorescence intensity of HTFMC is pronounced; the signal from the MitoTracker® red begins to decrease and the first signs of apoptotic blebbling can also be observed on cell surfaces (Figure 3). For hMSCs dosed with 20 irradiations of excitation light the signal from HTMFC was intensified further, suggesting sub-cellular spaces were being enriched with ROS. In addition, the MitoTracker® red emission was greatly diminished, implying that the number of active mitochondrial membrane potentials was reduced; and there are more signs of a decline in cellular viability as bright field images showed signs of increases in apoptotic blebbing (Figure 3).

Quantification of the effects of controlled intracellular ROS generation on cellular viability and hMSCs characterisation

Flow cytometry was employed to quantify the viability and any phenotypic variation in hMSC populations treated with Zn (II) porphyrin functionalised nanoparticles and after illumination with repeated doses of light (produced using a custom designed irradiator that replicated the power and wavelength of excitation light used during fluorescence microscopy, see supporting information). Cell viability, apoptosis (controlled cell death), necrosis (uncontrolled cell death), and cellular differentiation were investigated through the use of fluorescent probes. Apoptosis was investigated using Annexin V Alexa Flour® 488, which binds to cell surface markers that are translocated during apoptosis.[35] Whereas, necrosis was determined using the DNA intercalator propidium iodide, which stains deteriorating cells with permeable membranes.[36] The effect of intracellular ROS on hMSCs phenotype was studied using fluorescent antibodies for specific cell surface markers.[37, 38]

Controlled apoptotic and uncontrolled necrotic cell death

Figure 4 shows there are no significant differences in the percentage of apoptotic and necrotic cells for 1) untreated and 2) Cu (II) porphyrin functionalised nanoparticle treated hMSC populations, after irradiation with 5 to 20 doses of excitation light (approximately 20% of the population express markers for apoptotic events that can be attributed to cell death during storage and thawing). However, hMSCs treated with Zn (II) porphyrin functionalised particles demonstrate statistically significant increases in the population of apoptotic cells when compared to 1) untreated and Cu(II) functionalised nanoparticle treated hMSCs ($p<0.05$) and 2) after repeated irradiation with excitation light ($p<0.001$). Dosing hMSCs with 5, 10, 15 and 20 irradiations of excitation light increases the percentage of apoptotic cells to 29 %, 30 %, 37 % and 44 %, respectively (n=6). We postulate that the percentage of apoptotic cells does not increase at low irradiation levels due to the natural antioxidant levels present in the cell.[34] However, once this antioxidant reservoir is exhausted it is noticeable the percentage of apoptotic cells increases linearly with light irradiations.

Populations of untreated hMSCs and Cu (II) or Zn (II) porphyrin functionalised nanoparticles treated hMSCs contained low levels of propidium iodine positive cells; less than 5% of total population, Figure 4. There were no significant differences between the hMSC populations after repeated doses of excitation light, from 5 to 20 irradiations. These findings suggest repeated irradiation of internalised Zn (II) porphyrin functionalised nanoparticles generate doses of ROS that signal hMSCs to undergo controlled apoptotic cell death rather than uncontrolled necrotic cell death. These observations also mirror findings observed in Figure 3, which show signs of apoptotic blebbing, rather than necrotic cell lysis.

hMSC differentiation

Phenotypic characterisation of hMSCs was explored, by fluorescently labelling cell surface markers with antibodies, after 20 irradiations of excitation light and two cellular passages. Phenotypic characterisation of hMSCs showed untreated hMSCs and, Cu (II) or Zn (II) porphyrin functionalised nanoparticle treated hMSCs presented virtually identical phenotypic profiles (see supporting information Figure S9 & S10). These results suggest that irradiation of Zn (II) porphyrin functionalised nanoparticles and subsequent ROS generation does not change the phenotype or induce senescence patterns in hMSCs.

Conclusion

We have demonstrated nanoparticles functionalised with Zn (II) porphyrin trigger intracellular ROS production. The intracellular effects of enhanced ROS production were evidenced through visualisation using BPTFMC, which is transformed into fluorescent HTMFC in the presence of H_2O_2, and observation of diminishing mitochondrial membrane potentials, using MitoTracker® red. Increases in: 1) the percentage of Zn (II) porphyrin conjugated to nanoparticles, from 5 % to 20 %, and 2) the number of irradiations of excitation light, enhanced ROS production and subsequent cytotoxicity. Controlled irradiation of Zn (II) porphyrin functionalised nanoparticles was found to signal apoptosis in hMSCs, but did not induce necrosis or phenotypic changes in hMSC subcultures. We anticipate porphyrin functionalised nanoparticles will prove to be a valuable tool to generate controlled amounts of intracellular ROS to advance the study of cellular processes and disease progression.

References

1. Apel, K.; Hirt, H., Reactive oxygen species: Metabolism, oxidative stress, and signal transduction. *Annual Review of Plant Biology* 2004, 55, 373-399.
2. Turrens, J. F., Mitochondrial formation of reactive oxygen species. *Journal of Physiology-London* 2003, 552, 335-344.
3. Karihtala, P.; Soini, Y., Reactive oxygen species and antioxidant mechanisms in human tissues and their relation to malignancies. *Apmis* 2007, 115, 81-103.
4. Simon, H. U.; Haj-Yehia, A.; Levi-Schaffer, F., Role of reactive oxygen species (ROS) in apoptosis induction. *Apoptosis* 2000, 5, 415-418.
5. Torres, M. A.; Jones, J. D. G.; Dangl, J. L., Reactive oxygen species signaling in response to pathogens. *Plant Physiology* 2006, 141, 373-378.
6. Liu, Y. B.; Fiskum, G.; Schubert, D., Generation of reactive oxygen species by the mitochondrial electron transport chain. *Journal of Neurochemistry* 2002, 80, 780-787.
7. Kamiya, H., Mutagenic potentials of damaged nucleic acids produced by reactive oxygen/nitrogen species: approaches using synthetic oligonucleotides and nucleotides. *Nucleic Acids Research* 2003, 31, 517-531.
8. Berlett, B. S.; Stadtman, E. R., Protein oxidation in aging, disease, and oxidative stress. *Journal of Biological Chemistry* 1997, 272, 20313-20316.
9. Aitken, R. J.; Clarkson, J. S.; Fishel, S., GENERATION OF REACTIVE OXYGEN SPECIES, LIPID-PEROXIDATION, AND HUMAN-SPERM FUNCTION. *Biology of Reproduction* 1989, 41, 183-197.
10. Festjens, N.; Vanden Berghe, T.; Vandenabeele, P., Necrosis, a well-orchestrated form of cell demise: Signalling cascades, important mediators and concomitant immune response. *Biochimica Et Biophysica Acta-Bioenergetics* 2006, 1757, 1371-1387.
11. Waris, G.; Ahsan, H., Reactive oxygen species: role in the development of cancer and various chronic conditions. *Journal of carcinogenesis* 2006, 5, 14-14.
12. Uttara, B.; Singh, A. V.; Zamboni, P.; Mahajan, R. T., Oxidative Stress and Neurodegenerative Diseases: A Review of Upstream and Downstream Antioxidant Therapeutic Options. *Current Neuropharmacology* 2009, 7, 65-74.
13. Forman, H. J., Use and abuse of exogenous H_2O_2 in studies of signal transduction. *Free Radical Biology and Medicine* 2007, 42, 926-932.
14. de Oliveira-Marques, V.; Cyrne, L.; Marinho, H. S.; Antunes, F., A quantitative study of NF-kappa B activation by H2O2: Relevance in inflammation and synergy with TNF-alpha. *Journal of Immunology* 2007, 178, 3893-3902.
15. Miller, E. W.; Dickinson, B. C.; Chang, C. J., Aquaporin-3 mediates hydrogen peroxide uptake to regulate downstream intracellular signaling. *Proceedings of the National Academy of Sciences of the United States of America* 2010, 107, 15681-15686.

16. Huang, B. K.; Sikes, H. D., Quantifying intracellular hydrogen peroxide perturbations in terms of concentration. *Redox Biology* 2014, 2, 955-962.
17. Aylott, J. W., Optical nanosensors - an enabling technology for intracellular measurements. *Analyst* 2003, 128, 309-312.
18. Desai, A. S.; Chauhan, V. M.; Johnston, A. P. R.; Esler, T.; Aylott, J. W., Fluorescent nanosensors for intracellular measurements: synthesis, characterization, calibration, and measurement. *Frontiers in physiology* 2013, 4, 401-401.
19. Benjaminsen, R. V.; Sun, H.; Henriksen, J. R.; Christensen, N. M.; Almdal, K.; Andresen, T. L., Evaluating Nanoparticle Sensor Design for Intracellular pH Measurements. *Acs Nano* 2011, 5, 5864-5873.
20. Chauhan, V. M.; Burnett, G. R.; Aylott, J. W., Dual-fluorophore ratiometric pH nanosensor with tuneable pK(a) and extended dynamic range. *Analyst* 2011, 136, 1799-1801.
21. Giuntini, F.; Chauhan, V. M.; Aylott, J. W.; Rosser, G. A.; Athanasiadis, A.; Beeby, A.; MacRobert, A. J.; Brown, R. A.; Boyle, R. W., Conjugatable water-soluble Pt(II) and Pd(II) porphyrin complexes: novel nano-and molecular probes for optical oxygen tension measurement in tissue engineering. *Photochemical & Photobiological Sciences* 2014, 13, 1039-1051.
22. Lee, Y. E. K.; Smith, R.; Kopelman, R., Nanoparticle PEBBLE Sensors in live cells and in vivo. *Annual Review of Analytical Chemistry* 2009, 2, 57-76.
23. Coupland, P. G.; Briddon, S. J.; Aylott, J. W., Using fluorescent pH-sensitive nanosensors to report their intracellular location after Tat-mediated delivery. *Integrative Biology* 2009, 1, 318-323.
24. Clark, H. A.; Hoyer, M.; Philbert, M. A.; Kopelman, R., Optical nanosensors for chemical analysis inside single living cells. 1. Fabrication, characterization, and methods for intracellular delivery of PEBBLE sensors. *Analytical Chemistry* 1999, 71, 4831-4836.
25. Doussineau, T.; Schulz, A.; Lapresta-Fernandez, A.; Moro, A.; Koersten, S.; Trupp, S.; Mohr, G. J., On the Design of Fluorescent Ratiometric Nanosensors. *Chemistry-a European Journal* 2010, 16, 10290-10299.
26. Chauhan, V. M.; Orsi, G.; Brown, A.; Pritchard, D. I.; Aylott, J. W., Mapping the Pharyngeal and Intestinal pH of Caenorhabditis elegans and Real-Time Luminal pH Oscillations Using Extended Dynamic Range pH-Sensitive Nanosensors. *ACS nano* 2013, 7, 5577-87.
27. Kuruppuarachchi, M.; Savoie, H.; Lowry, A.; Alonso, C.; Boyle, R. W., Polyacrylamide Nanoparticles as a Delivery System in Photodynamic Therapy. *Molecular Pharmaceutics* 2011, 8, 920-931.
28. Bonnett, R., PHOTOSENSITIZERS OF THE PORPHYRIN AND PHTHALOCYANINE SERIES FOR PHOTODYNAMIC THERAPY. *Chemical Society Reviews* 1995, 24, 19-33.
29. Papkovsky, D. B.; O'Riordan, T. C., Emerging applications of phosphorescent metalloporphyrins. *Journal of Fluorescence* 2005, 15, 569-584.
30. Pavani, C.; Uchoa, A. F.; Oliveira, C. S.; Iamamoto, Y.; Baptista, M. S., Effect of zinc insertion and hydrophobicity on the membrane interactions and PDT activity of porphyrin photosensitizers. *Photochemical & Photobiological Sciences* 2009, 8, 233-240.
31. Giuntini, F.; Dumoulin, F.; Daly, R.; Ahsen, V.; Scanlan, E. M.; Lavado, A. S. P.; Aylott, J. W.; Rosser, G. A.; Beeby, A.; Boyle, R. W., Orthogonally bifunctionalised polyacrylamide nanoparticles: a support for the assembly of multifunctional nanodevices. *Nanoscale* 2012, 4, 2034-2045.
32. Szintay, G.; Horvath, A., Five-coordinate complex formation and luminescence quenching study of copper(II) porphyrins. *Inorganica Chimica Acta* 2001, 324, 278-285.

33. Pendergrass, W.; Wolf, N.; Poot, M., Efficacy of MitoTracker Green (TM) and CMXRosamine to measure changes in mitochondrial membrane potentials in living cells and tissues. *Cytometry Part A* 2004, 61A, 162-169.
34. Yagi, H.; Tan, J.; Tuan, R. S., Polyphenols suppress hydrogen peroxide-induced oxidative stress in human bone-marrow derived mesenchymal stem cells. *Journal of Cellular Biochemistry* 2013, 114, 1163-1173.
35. Vermes, I.; Haanen, C.; Steffensnakken, H.; Reutelingsperger, C., A NOVEL ASSAY FOR APOPTOSIS - FLOW CYTOMETRIC DETECTION OF PHOSPHATIDYLSERINE EXPRESSION ON EARLY APOPTOTIC CELLS USING FLUORESCEIN-LABELED ANNEXIN-V. *Journal of Immunological Methods* 1995, 184, 39-51.
36. Sawai, H.; Domae, N., Discrimination between primary necrosis and apoptosis by necrostatin-1 in Annexin V-positive/propidium iodide-negative cells. *Biochemical and Biophysical Research Communications* 2011, 411, 569-573.
37. Gaebel, R.; Furlani, D.; Sorg, H.; Polchow, B.; Frank, J.; Bieback, K.; Wang, W.; Klopsch, C.; Ong, L.-L.; Li, W.; Ma, N.; Steinhoff, G., Cell Origin of Human Mesenchymal Stem Cells Determines a Different Healing Performance in Cardiac Regeneration. *Plos One* 2011, 6.
38. Jones, E. A.; Kinsey, S. E.; English, A.; Jones, R. A.; Straszynski, L.; Meredith, D. M.; Markham, A. F.; Jack, A.; Emery, P.; McGonagle, D., Isolation and characterization of bone marrow multipotential mesenchymal progenitor cells. *Arthritis and Rheumatism* 2002, 46, 3349-3360.

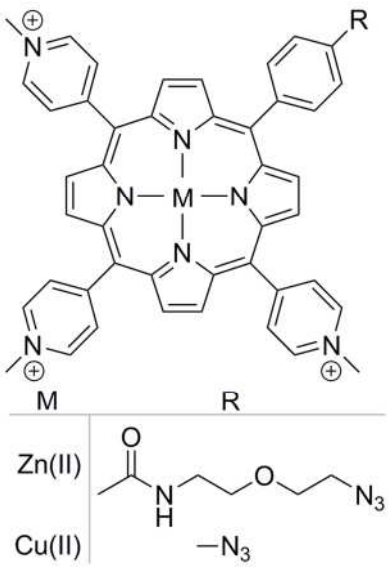

Scheme 1. Chemical structure of azide functionalised cationic porphyrin with zinc (II) and copper (II) metal centres.

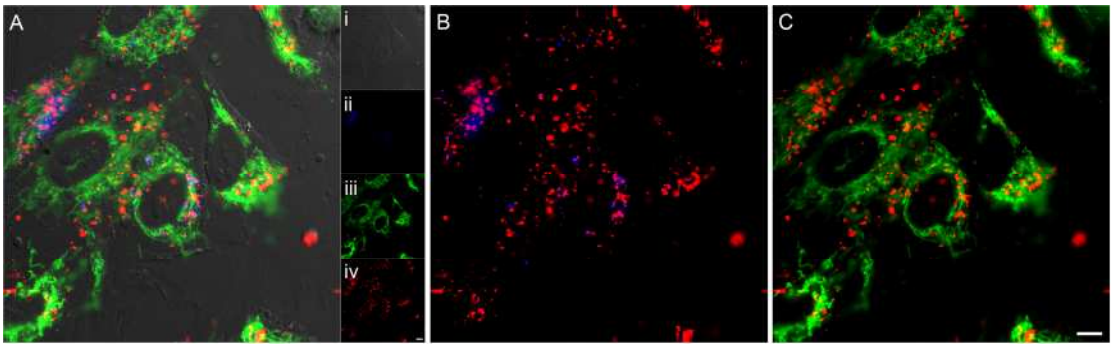

Figure 1. (A) Merged fluorescence image of (Ai) bright-field image of hMSCs treated with (Aii) LysoTracker® blue, (Aiii) MitoTracker®green and (Aiv) Zn(II) porphyrin conjugated nanoparticles (*red*). Co-localisation analysis between (B) Zn(II) porphyrin conjugated nanoparticles and LysoTracker® blue, and (C) Zn(II) porphyrin conjugated nanoparticles and MitoTracker®green. Scale bar = 10 µm.

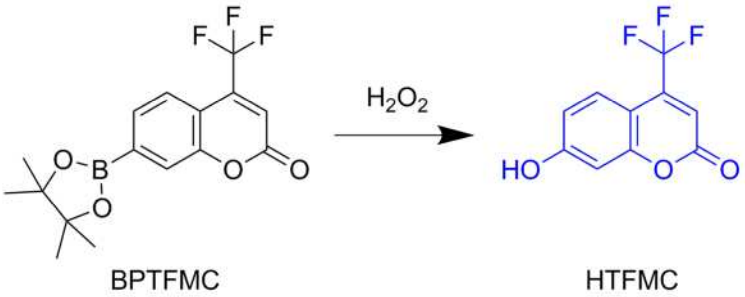

Scheme 1. Reaction between non-fluorescent 7-(4,4,5,5-tetramethyl-1,3,2-dioxaborolan-2-yl)-4-(trifluoromethyl)-2H-chromen-2-one (BPTFMC) and ROS producing fluorescent -hydroxy-4-(trifluoromethyl)-2H-chromen-2-one (HTFMC). HTFMC peak excitation and emmsion wavelengths are 395 nm and 435 nm, respectively.

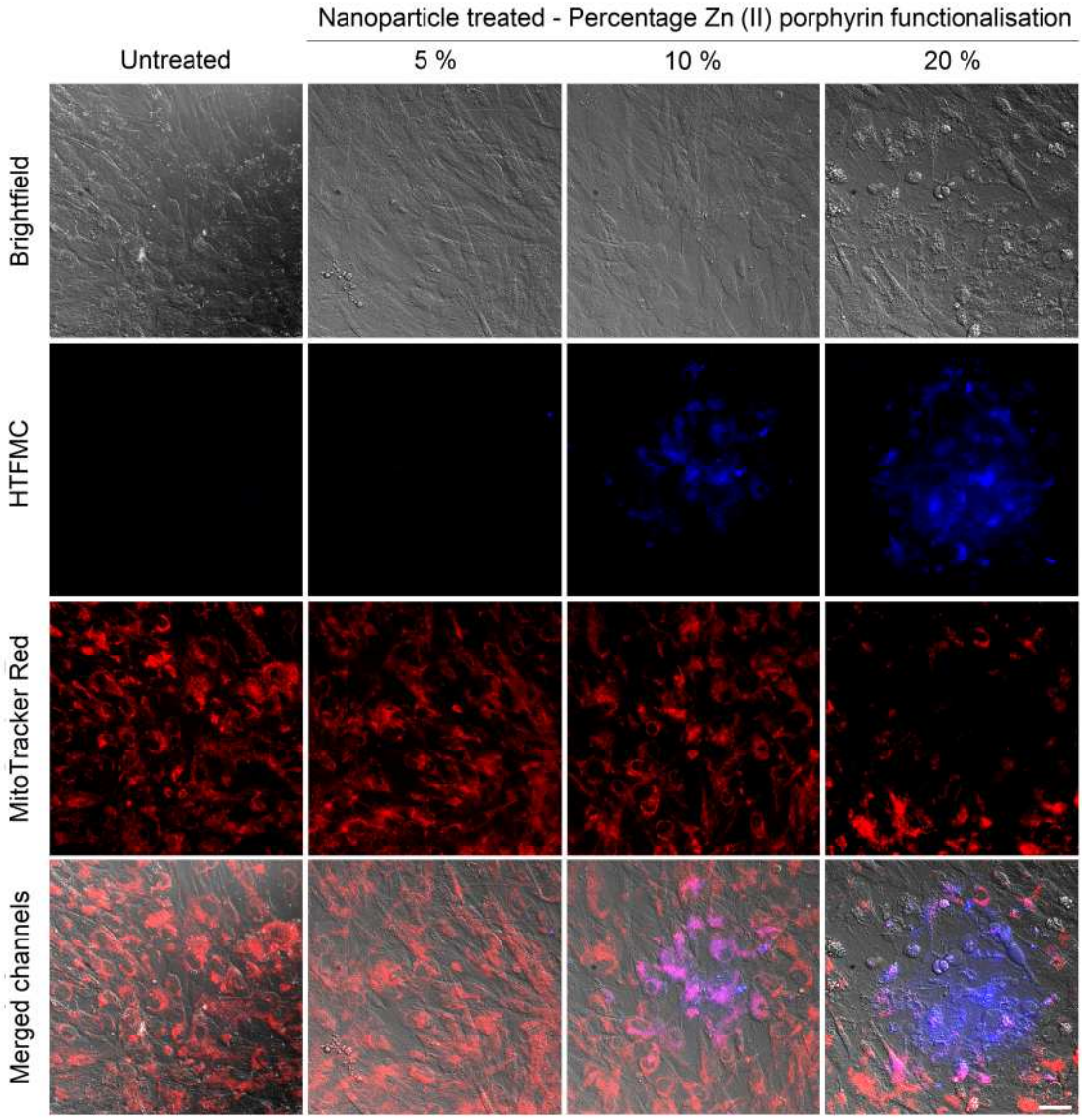

Figure 2. Bright-field and fluorescence images of untreated hMSCs and hMSCs treated with 5, 10 and 20 % Zn(II) functionalised nanoparticles, stained with BPTFMC and MitoTracker Red, irradiated with a single dose of light. BPTFMC, in the presence of H_2O_2, is converted to fluorescent HTMFC. Scale bar = 50 µm.

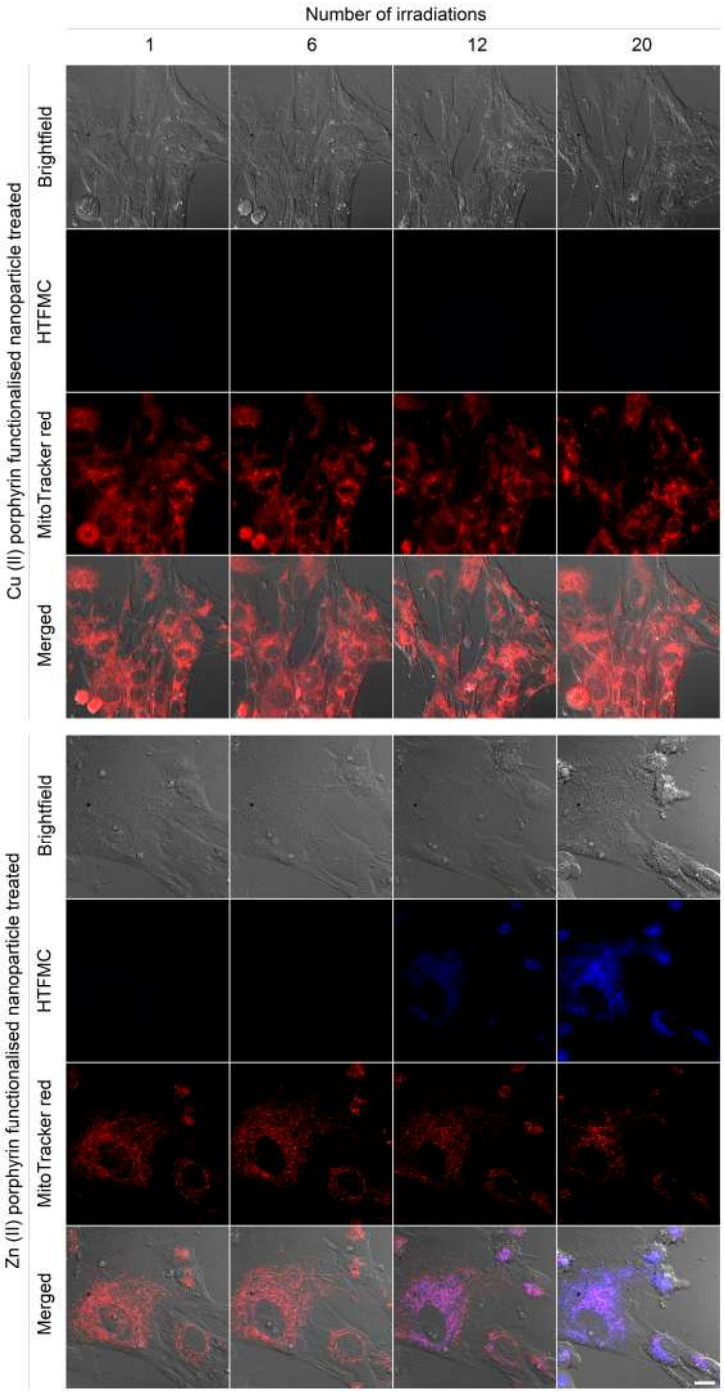

Figure 3. (1) Merged bright-field and fluorescence images of hMSCs with internalised Cu(II) (control) and Zn(II) functionalised nanoparticles (photosensitiser) and (2) merged fluorescence images of hMSCs stained with BPTFMC and MitoTracker® red. Green, blue and red fluorescence are indicative of (1) nanoparticle location, (2) HTFMC production and subsequent ROS production and (3) active mitochondrial membrane potentials and cell viability. Scale bar = 20 µm.

522
523

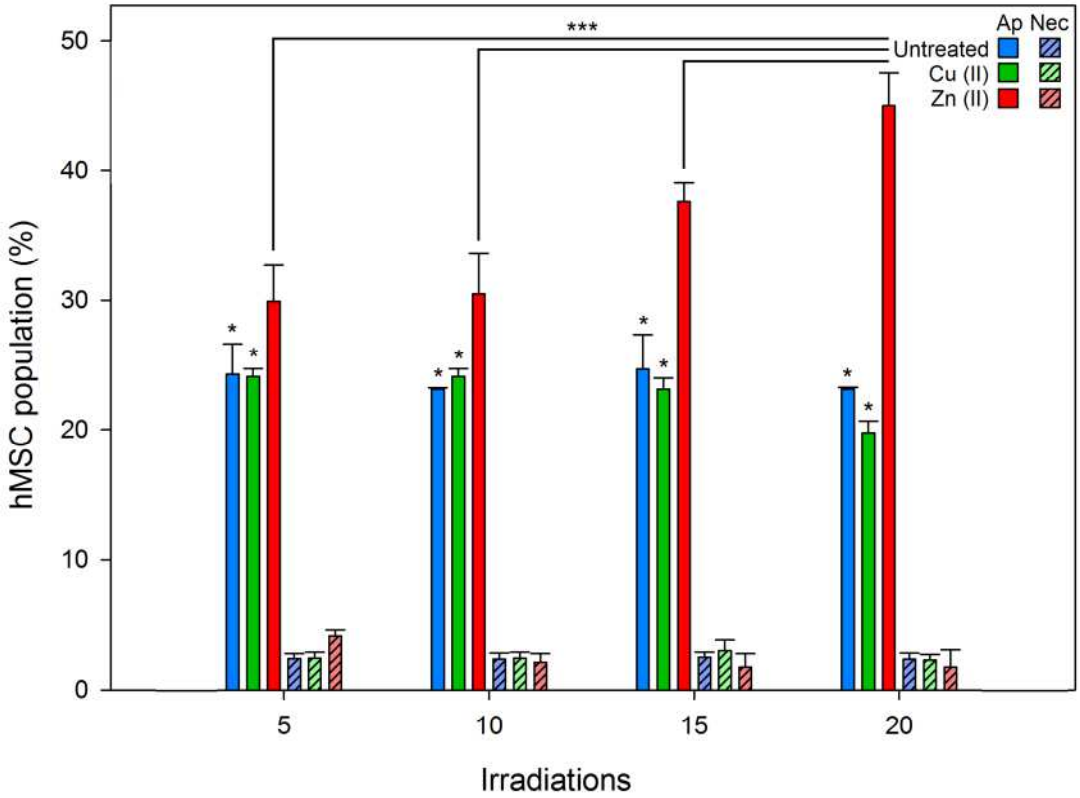

524
525
526 **Figure 4.** Comparison of untreated (*blue*) and 5% Cu (II) (*green*) or 5% Zn (II) (*red*)
527 functionalised nanoparticle treated hMSC populations undergoing apoptosis (*Ap*, *solid*) and
528 necrosis (*Nec*, *diagonal lines*) after 5, 10, 15 and 20 irradiations of excitation light.
529 Percentage of apoptosis and necrosis was determined using flow cytometry by staining
530 apoptotic hMSCs with Annexin V 488 and propidium iodide, respectively. Error bars
531 represent standard deviation from the mean (n=6). One Way ANOVA *** = $p < 0.001$; One
532 way ANOVA * = $p < 0.05$. *P* values less than 0.05 were considered statistically different.
533